

Provided for non-commercial research and education use.  
Not for reproduction, distribution or commercial use.



This article appeared in a journal published by Elsevier. The attached copy is furnished to the author for internal non-commercial research and education use, including for instruction at the authors institution and sharing with colleagues.

Other uses, including reproduction and distribution, or selling or licensing copies, or posting to personal, institutional or third party websites are prohibited.

In most cases authors are permitted to post their version of the article (e.g. in Word or Tex form) to their personal website or institutional repository. Authors requiring further information regarding Elsevier's archiving and manuscript policies are encouraged to visit:

<http://www.elsevier.com/authorsrights>



Contents lists available at ScienceDirect

## Behavioural Brain Research

journal homepage: [www.elsevier.com/locate/bbr](http://www.elsevier.com/locate/bbr)

## Research report

# Tripchlorolide improves age-associated cognitive deficits by reversing hippocampal synaptic plasticity impairment and NMDA receptor dysfunction in SAMP8 mice



Nan Lin<sup>a,b,1</sup>, Xiao-dong Pan<sup>a,b,1</sup>, Ai-qin Chen<sup>b</sup>, Yuan-gui Zhu<sup>a,b</sup>, Ming Wu<sup>a,b</sup>,  
Jing Zhang<sup>a,b</sup>, Xiao-chun Chen<sup>a,b,\*</sup>

<sup>a</sup> Department of Neurology, Fujian Institute of Geriatrics, Fujian Medical University Union Hospital, 29 Xinquan Road, Fuzhou 350001, China

<sup>b</sup> Key Laboratory of Brain Aging and Neurodegenerative Disease, Fujian Key Laboratory of Molecular Neurology, Fujian Medical University, 29 Xinquan Road, Fuzhou 350001, China

## HIGHLIGHTS

- A novel extract of natural herbal, tripchlorolide has anti-dementia action.
- Long-term T<sub>4</sub> treatment prevents learning and memory loss in aged SAMP8 mice.
- T<sub>4</sub> ameliorates hippocampal LTP in aged SAMP8 mice.
- T<sub>4</sub> alleviates synaptic plasticity dysfunction of the hippocampus.
- T<sub>4</sub> intensified the signal pathway of CaMKII-CREB-BDNF in SAMP8 mice.

## ARTICLE INFO

## Article history:

Received 4 June 2013

Received in revised form

29 September 2013

Accepted 3 October 2013

Available online 17 October 2013

## Keywords:

Tripchlorolide

Aging

Cognition

Long-term potentiation

Synaptic plasticity

NMDA receptor

## ABSTRACT

Deficits in cognition and performance accompanying age-related neurodegenerative diseases such as Alzheimer's disease (AD) are closely associated with the impairment of synaptic plasticity. Here, using a mouse model of senescence-accelerated P8 (SAMP8), we reported the role of tripchlorolide (T<sub>4</sub>), an extract of the natural herb *Tripterygium wilfordii Hook F*, in improving cognitive deficits and promoting the long-term potentiation (LTP) of hippocampal slices via the N-methyl-D-aspartate receptor (NMDAR)-dependent signaling pathway. Our results demonstrated that chronic administration of T<sub>4</sub> at low doses (0.25, 1.0, or 4.0 μg/kg per day, injected intraperitoneally for 75 days) significantly improved learning and memory function in aged SAMP8 mice, as indicated by a chain of behavioral tests including the Y-maze and Morris water maze. Additionally, T<sub>4</sub> reversed the impaired LTP in hippocampal CA1 regions of SAMP8 mice in a dose-dependent manner. Moreover, it upregulated the levels of phospho-NMDAR1, postsynaptic density-95 (PSD-95), phospho-calcium-calmodulin dependent kinase II (CaMKII), phospho-CREB and brain derived neurotrophic factor (BDNF) in the hippocampus. This indicates that T<sub>4</sub> prevents the impairment of NMDAR-mediated synaptic plasticity-related signal molecules. At optimal doses, T<sub>4</sub> did not show significant side-effects on blood counts, blood biochemical measures, or survival of the mice. This novel mechanism in reversing age-related synaptic dysfunction and NMDAR functional deficits suggests that T<sub>4</sub> can halt the manifestation of a key early-stage event in AD. With the consideration of SAMP8 mice as a model to develop therapeutic interventions for AD, our findings provide new insight into the clinical application of tripchlorolide in AD treatment.

© 2013 Elsevier B.V. All rights reserved.

**Abbreviations:** AD, Alzheimer's Disease; BDNF, brain-derived neurotrophic factor; CaMKII, calcium/calmodulin-dependent protein kinase II; CREB, cyclic AMP-response element binding protein; EPSPs, excitatory postsynaptic potentials; LTP, long-term potentiation; MWM, Morris water maze; NMDAR, N-methyl-D-aspartate receptor; PSD-95, postsynaptic density-95; SAMP8, senescence-accelerated mouse Prone 8 SAMR1; T<sub>4</sub>, tripchlorolide.

\* Corresponding author at: Department of Neurology, Fujian Medical University Union Hospital, 29 Xinquan Road, Fuzhou, Fujian 350001, China. Tel.: +86 591 8333 3995; fax: +86 591 8337 0393.

E-mail addresses: [chenxc998@mail.fjmu.edu.cn](mailto:chenxc998@mail.fjmu.edu.cn), [chenxc998@163.com](mailto:chenxc998@163.com) (X.-c. Chen).

<sup>1</sup> These authors contributed equally to this work and share first authorship.

## 1. Introduction

Age is the most prominent risk factor in neurodegenerative diseases including Alzheimer's disease (AD). In aged adults, AD is the most common cause of dementia, which manifests the signs of memory loss, spatial disorientation, and weakness of intellectual capacity [1]. In fact, this age-related decline in cognitive function is associated with increased synaptic function change in brain.

Of all the animal AD research models, the senescence-accelerated prone-8 (SAMP8) displays irreversible advancing early senescence and exhibits cognitive impairment that reduces physical activity and erodes memory and thinking skills as seen in AD patient [2]. Interestingly, SAMP8 mice exhibit not only the cognitive deficits with the underlying mechanisms in synaptic, dendritic and memory alterations [3,4], but also pathological changes similar to those found in AD, such as the abnormal expression of amyloid precursor protein (APP) and amyloid-beta (A $\beta$ ) proteins, amyloid-like deposition in the brain, and increased phosphorylation of Tau [5–8]. Different from other aged wild-type and single-transgenic (APP or PS1) and double-transgenic (APP + PS1) mice which present significant deficits in learning and long-term potentiation (LTP) properties that are not related with the presence of amyloid beta deposits [9], these mice have early amyloid accumulation in the hippocampus which then aggravates with age [6]. Both aging and A $\beta$  decrease the neuronal plasticity by targeting N-methyl-D-aspartate receptor (NMDAR), which can adversely impair the cognitive performance. This impaired cognitive performance in aged SAMP8 mice can be improved by antisense to APP and antibody to reduce the level of A $\beta$  in the brain [10–13]. In the early stage of AD, A $\beta$  accumulation is also documented and found to be associated with synaptic dysfunction. Taken together, these findings suggest that the abnormal expression of A $\beta$  contributes to the cognitive decline in aged SAMP8 mice and the animal model can be a useful tool to study the mechanisms underlying cognitive impairments and to explore the related drug treatments for AD [14].

Of all the candidate agents, tripchlorolide (designated as T<sub>4</sub>, Fig. 1) is a novel extract from Chinese herb *Tripterygium wilfordii* Hook F (TWHF) that has been found to have potent anti-inflammatory and immunosuppressive functions and is widely used in China for treatment of rheumatoid arthritis [15,16]. Compared with other analogs, T<sub>4</sub> has a lower toxicity [17], and its lipophilic properties generated by chloridion modification and small molecular size (MW 397) most likely facilitate its passage through the blood–brain barrier. Many studies including epidemiological, basic and clinical research on AD have shown that nonsteroidal anti-inflammatory drug (NSAID) treatment reduces the risk of AD. As an extract from Chinese herb TWHF, T<sub>4</sub> has been found to have a significant neuroprotective effect in combatting inflammatory neurotoxicity induced by lipopolysaccharide-activated microglia [18]. It can protect

neuronal cells not only from microglia-mediated A $\beta$  neurotoxicity by inhibiting NF- $\kappa$ B and JNK signaling [19], but also directly protect against the neuronal apoptosis induced by A $\beta$ , by regulating Wnt/ $\beta$ -catenin signaling [20]. Recently, in our studies on T<sub>4</sub>, we also found that T<sub>4</sub> attenuates the secreted A $\beta$ <sub>1–42</sub> and A $\beta$ <sub>1–40</sub> in N2a/APP695 cells (paper unpublished, data not shown). These studies suggest that T<sub>4</sub> could be a modulator in the production of A $\beta$  and a potential neurotrophic and neuroprotective agent in the treatment of AD.

Of the underlying mechanisms, synaptic loss and synaptic dysfunction are the most robust predictors of cognitive impairment in AD [21]. The pathogenesis of AD can be best explained by a loss of plasticity [22], which may have adverse dendritic ramifications, such as synaptic remodeling, long-term potentiation (LTP), axonal sprouting, neurite extension, synaptogenesis, and neurogenesis. To date, few studies have shown that NSAID could restore working memory deficit and decremental LTP and discussed the underlying mechanisms [23] and even scarce reports have focused on the role of T<sub>4</sub> in an age-related animal model with synaptic plasticity disruption, especially the effects of T<sub>4</sub> on LTP and synaptic plasticity-related proteins and the related signal activation. Here, we investigated the effects of long-term administration of T<sub>4</sub> on the improvement of learning and memory dysfunction in aged SAMP8 mice. Furthermore, we elucidated that T<sub>4</sub> that preserves the synaptic plasticity through regulating LTP and synaptic plasticity-related proteins including postsynaptic density-95 (PSD-95), and NMDAR. In addition, we observe the effect of long-term administration of T<sub>4</sub> at an optimal dose on the survival of mice and drug side-effects on blood counts and blood biochemical changes.

## 2. Materials and methods

### 2.1. Reagents

T<sub>4</sub> was obtained from Department of Pharmacology of Fudan University (Shanghai, China). The material was in the form of white needle-like crystals, with a melting point of 256–258°C, a molecular weight of 397, and a purity of 98% by reverse phase high-pressure liquid chromatography (HPLC) evaluation.

### 2.2. Animals and treatment with

Virgin male SAMP8 and SAMR1 mice were generously provided by the Department of Laboratory Animal Science of Peking University. Each mouse was individually housed in a plastic cage with a constant temperature of 22 ± 0.5°C and humidity of 60 ± 5% under a 12h light–dark cycle (lights turned on at 6:00 a.m.). All mice received standard rodent diet and tap water *ad lib*. Any animals with gross defects (tumors outside trunk, motor incapacitation, or overt blindness) were excluded prior to the behavioral examination. All procedures used in these studies observed the National Institute of Health Guidelines for the Care and Use of Laboratory Animals and were approved by the Institutional Animal Care and Utilization Committee of Fujian Medical University.

Mice were allowed 1 week to adapt to their environment after arrival. Before the being used for experiments, SAMP8 mice were tested in a Y-maze and then randomly allocated into four groups of 18–20, according to their Y-maze performance.

T<sub>4</sub> was prepared fresh and applied as a single daily injection at 9:00 a.m. It was first dissolved in dimethylsulphoxide (DMSO) and later diluted with 0.9% NaCl–physiological saline (N.S.) (DMSO < 0.05%). A single daily dose of 0.25, 1.0 and 4.0  $\mu$ g/kg was respectively administered to SAMP8 mice aged 7.5 months for a total of 75 days. SAMP8 mice receiving vehicle (N.S.) were treated as a T<sub>4</sub>-free control. The age-matched

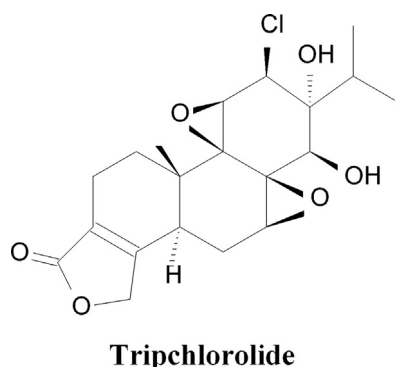


Fig. 1. The chemical structure of tripchlorolide (T<sub>4</sub>).

SAM-resistant/1 (SAMR1) mice treated with vehicle (N.S.) served as a model (SAMP8) control. During the experiment, animal weights were measured once per week. By the time for behavioral tests, all five groups of animals were 10 months old and were subjected to behavioral testing as described below.

### 2.3. Behavioral test

#### 2.3.1. Y-maze

**2.3.1.1. Apparatus.** Testing was performed in a Y-shaped maze as previously described [24]. The Y maze consisted of three plexiglass arms of equal size joined together in a Y configuration with the following dimensions: arm length 40 cm, height 25 cm, and width 10 cm. The apparatus was placed on the floor of the experimental room and illuminated with a 100-W bulb from 200 cm above.

**2.3.1.2. Spontaneous alternation.** This method was used to assess the normal navigation behaviors of rodents (without food deprivation or other aversive procedures). Mice were placed into the end of one arm and allowed to explore the maze freely for 8 min. All arm entries were sequentially scored so that the total number of arm entries, as well as the sequence of entries was recorded. The percentage of spontaneous alternation behavior was calculated as the number of trials containing entries into all three arms divided by the maximum possible alternations (the total number of arms entered minus 2) [25]. Additionally, the number of arm entries served as an indicator of activity.

**2.3.1.3. A two-trial recognition Y-maze.** The Y-maze has also been employed for the *Spatial* recognition memory test as described by Delli [26]. As in the aforementioned study, the Y-maze in the current paper consisted of three equilaterally intersecting arms with spatial cues positioned inside the maze and one trial consisted of two exposures to the maze. The mice were placed in an arm of the Y-maze (start arm) with one of the arms blocked off (novel arm) and were allowed to explore the start arm and remaining arm (other arm) for 10 min. And then they were removed from the maze and returned to their home cages. After a delay of 4 h, they were reintroduced to the spatial location where they had been placed in the first exposure and allowed to explore all three arms for 5 min, and the number of entries and time spent in each arm were recorded. The maze was wiped clean with 70% ethanol between each exposure to minimize odor cues. As reported by Conrad [27], mice with functional spatial memory are more likely to enter the arm located in the unexplored spatial location than to enter the arms in locations that they had already visited in the initial exposure, whereas mice with impaired spatial memory will explore the visited and unvisited arms similarly. It has been proposed that the duration of time animals spend in the novel arm reflects the exploratory behavior and while the number of entries into the novel arm, the inquisitive behavior [28,29].

**2.3.1.4. Contextual conditioned shock-light-dark task.** The floor of the Y-maze was electrified so that shocks ( $40 \pm 5$  V for 10 s) could be delivered. The arms of the Y-maze were designated 'start', 'correct' and 'incorrect', and the 'correct' arm remained illuminated throughout the test to encourage entry. The 'incorrect' arm remained electrified to discourage entry. At the beginning of the test, mice were placed in the start arm and three doors opened simultaneously to allow entry to all three arms of the Y-maze. An electric shock was delivered to induce escape from the start arm after the 'correct' arm had been illuminated for 5 s, causing entry into either the correct (illuminated) or incorrect (electrified) arm, which was scored as one trial. A total of 40 trials per day were carried out for each animal. In the first trial, one arm was designated as the start arm, a second arm as the correct and the remaining one

as the incorrect arm. In the next trial, the original start arm served as the incorrect arm, the original correct arm as the start arm, and the original incorrect arm as the correct one, and then the process was repeated. The inter-trial interval was 5 s. Retention was tested 24 h later. Each entry into the electrified arm was counted as an error, and the number of errors and the escape latency to the correct arm were used as parameters of hippocampal-dependent spatial learning memory.

#### 2.3.2. Morris water maze test

After the Y-maze test, the Morris water maze (MWM) was used as a method to evaluate of spatial learning and memory. The procedures were modified from Morris [30]. Briefly, a black circular tank (120 cm in diameter, 50 cm in height) filled with water ( $21\text{--}23$  °C) was circled by a white cloth curtain with four differently shaped (circle, triangle, square and column bar) black cardboard pieces hung equidistantly. A hyaline platform (10 cm in diameter, 24 cm in height) was submerged 1.0 cm below the surface of the water. Each mouse underwent four successive trials a day for 7 days in memory acquisition trials (training). The interval between trials every day was 15 min for the mice to recover physically. The sequence of water-entry points differed each day, but the location of the platform was constant. Latency to find the platform was measured up to a maximum of 60 s. On locating the platform, the mouse was left there for 15 s before the next trial. If the mouse failed to locate the platform within 60 s, it was guided to the platform and allowed to stay there for 15 s. Latency was recorded for each trial. A probe trial was performed 24 h after the last training session. In this trial, the platform was removed from the tank and mice were allowed to swim freely for 60 s. Two indexes were calculated: (1) the time (in s) spent by the mouse in the target quadrant in which the platform was hidden during acquisition trials; (2) the number of mice crossing exactly over the original position of the platform. All trials were videotaped by a camera located 2 m above the water surface and analyzed by a PC computer.

### 2.4. Hippocampal slice electrophysiology

#### 2.4.1. Hippocampus slice preparation

Mice were anesthetized with halothane and decapitated. Brains were rapidly removed, and transverse slices (500  $\mu$ m thick) of the hippocampus were cut from tissue blocks with a Vibratome (Technical Products International, Saint Louis, MO, USA). The slices were pre-incubated in an incubation chamber with oxygenated artificial cerebrospinal fluid (ACSF) at room temperature for at least 1 h before use. The ACSF containing (in mM) 117 NaCl, 4.7 KCl, 2.5  $\text{CaCl}_2$ , 1.2  $\text{MgCl}_2$ , 1.2  $\text{NaH}_2\text{PO}_4$ , 25  $\text{NaHCO}_3$ , and 11 glucose was continuously bubbled with 95%  $\text{O}_2$ /5%  $\text{CO}_2$  to maintain a pH of 7.4.

#### 2.4.2. Field-potential recordings

Slices were transferred to an interface chamber that was continually superfused with ACSF at a rate of 1–2 ml/min. Microelectrodes for extracellular recording were pulled from microfiber-filled borosilicate capillaries (OD 1.0 mm, ID 0.58 mm) using a Flaming–Brown horizontal micropipette puller (Sutter Instruments, Novato, CA, USA). The microelectrodes were filled with 3 M NaCl and the resistance was 3–5 M $\Omega$ . The microelectrode tips were visually positioned in the dendritic layer of the CA1 region using a dissecting microscope. A bipolar electrode was placed in the stratum radiatum to stimulate the Schaffer collateral/commissural pathway. The stimulus intensity was set to evoke 40–50% of the maximal amplitude of field excitatory postsynaptic potentials (EPSPs). The two train high frequency stimulation (100 Hz, 1 s) was delivered to induce LTP. Field EPSPs were monitored and analyzed with the use of a computer-based data acquisition system. The slopes of field EPSPs were normalized to the averaged baseline

value (100%). Only a single slice from each hippocampus was used for each group of experiments.

### 2.5. Tissue preparation

After the behavioral test, all animals were anesthetized with 10% chloral hydrate (3 ml/kg). Intracardiac blood was obtained for blood examination, and then mice from each group were perfused via the left ventricle with 30 ml of cold (4 °C) 0.1 M phosphate. The hippocampi were dipped into liquid nitrogen after a quick separation and then stored at –80 °C for western blotting.

### 2.6. Western blotting

The hippocampi were sonicated in a cold lysis buffer with protease inhibitors (lysed in a buffer containing 0.1 M TBS, 2.5 mM Na<sub>4</sub>P<sub>2</sub>O<sub>5</sub>·10H<sub>2</sub>O, 4 mM NaF, 2 mM Na<sub>3</sub>VO<sub>4</sub>·12H<sub>2</sub>O, 1% protease inhibitor cocktail, 1% Triton X-100). After 30 min on ice, the samples were centrifuged at 16,000 × g for 10 min at 4 °C. The supernatants were collected gently, and a fraction of the total homogenates was removed for measurement of total protein concentrations. A total of 60 µg protein lysates were separated with 10% sodium dodecyl sulfate–polyacrylamide gel electrophoresis (SDS–PAGE) (Bio-Rad Laboratories, Foster City, CA, USA) and transferred onto polyvinylidene difluoride (PVDF) transfer membranes (Millipore, Billerica, MA, USA). After blocked in a 5% non-fat dry milk solution, the membranes were incubated overnight at 4 °C with different antibodies: rabbit monoclonal PSD-95 (Millipore, Billerica, MA, USA, 1:1000), p-NMDAR1 (Ser896) (Santa Cruz, Dallas, TX, USA, 1:200), p-CaMKII (Thr286) (Santa Cruz, Dallas, TX, USA, 1:2000), CREB (Cell Signaling Technology, Beverly, MA, USA, 1:1000), p-CREB (Ser133) (Cell Signaling Technology, Beverly, MA, USA, 1:1000), and BDNF (Santa Cruz, Dallas, TX, USA, 1:150). After 3 washes with TBST, the membranes were incubated for 90 min with horseradish peroxidase-coupled secondary antibody (KPL, Gaithersburg, MD, USA, 1:2000) at room temperature. Immunoreactive bands were visualized using an enhanced chemiluminescence kit (KPL, Gaithersburg, MD, USA). α-Tubulin (Sigma, Saint Louis, MO, USA, 1:8000) was used as an internal protein control. Immunoreactive signals were visualized on the X-ray film. Quantification of the band density was performed by densitometric analysis.

### 2.7. Blood examination

The blood counts for mice from each group were measured by a HEMAVET 950 veterinary multi-species hematology system (Anchorage, AK, USA). The serum biochemistry indexes were measured by BECKMAN LX20 clinical chemistry system (Brea, CA, USA).

### 2.8. Statistical analysis

Statistical analyses were performed using GraphPad Prism 4.03 and Sigmaplot 3.5. All data were expressed as “mean ± standard error mean (S.E.M)”. Indexes in acquisition trails such as escape latency in the water maze were analyzed by repeated-measure two-way ANOVA. The other behavior results and the expression of proteins were analyzed by ANOVA followed by Tukey's *post hoc* test. In electrophysiology experiments, statistical significance between groups was measured by one-way ANOVA followed by Bonferroni post-test across the postconditioning points on the LTP data sets and the statistical significance in every postconditioning point was assessed by Student's *t*-tests. Survival curves were analyzed by the Logrank test. The data of blood examination was analyzed by

one-way ANOVA. For all statistical analyses, *p* value of less than 0.05 was considered to be significant.

## 3. Results

### 3.1. Long-term treatment with T<sub>4</sub> alleviates learning and memory loss in aged SAMP8 mice

In an effort to test whether T<sub>4</sub> could ameliorate cognitive deficits in aged SAMP8 mice, 7.5-month-old SAMP8 mice were treated daily with T<sub>4</sub> (at 0.25, 1.0 and 4.0 µg/kg per day respectively, injected intraperitoneally for 75 days). SAMR1 mice of the same age were used as a “normal aging” control. Their performance in the Y-maze and Morris water maze was used to determine whether T<sub>4</sub> could improve their learning and memory function (by the time of behavioral tests, aged 10 months). SAMR1 mice of the same age acted as a “normal aging” control.

In the Y-maze test, the number of arm entries decreased significantly among vehicle-treated SAMP8 mice (Fig. 2A, *p* < 0.05, vs. SAMR1 group), which indicates the impairment of locomotion abilities and exploratory activities of aged SAMP8 mice. Spontaneous alternation represents spatial working memory, which is classified as short term and hippocampus-dependent memory [31] In this study, the 10-month-old SAMP8 mice showed a significant impairment in spontaneous alternation behavior when compared with to the age-matched SAMR1 group (Fig. 2B). Of note, the impairment was markedly recovered in the group of T<sub>4</sub>-treated aged SAMP8 mice and the ameliorative effect of T<sub>4</sub> was significant for any dose (0.25, 1.0 or 4.0 µg/kg per day) (Fig. 2B, *p* < 0.05). However, there were no observed dose-dependent effects.

We further tested visual recognition memory classified as hippocampus-dependent memory using a *Spatial* recognition memory test. When compared with SAMR1 mice, the vehicle-treated SAMP8 mice showed a significantly shortened exploratory time for the novel arm (Fig. 2C). In contrast, when compared with the vehicle-treated SAMP8 mice, the T<sub>4</sub>-treated aged SAMP8 mice showed a significant increase in the percentage of time spent in the novel arm (40.07% for 0.25 µg/kg per day, 35.85% for 1.0 µg/kg per day, and 40.38% for 4.0 µg/kg per day) (Fig. 2C).

Furthermore, the mice were tested by a contextual conditioned shock-light–dark task to evaluate their associative memory after treatment with T<sub>4</sub> and vehicle control. Vehicle-treated SAMP8 mice displayed a significant decrease in accuracy rate especially during the retention session (Fig. 2D) and displayed a longer escape latency (Fig. 2E), when compared with SAMR1 mice. As expected, T<sub>4</sub> treatment in the T<sub>4</sub>-treated aged SAMP8 mice resulted in a higher accuracy rate (over 90% for all three doses) and a shorter escape latency (below 10 s for all three doses) during acquisition and retention sessions (Fig. 2D and E).

Lastly, with the Morris water maze, we examined mice for spatial reference memory, which is classified as a long-term and hippocampus-dependent memory. In memory acquisition trials (training), the mice learned the hidden-platform task. The ability of SAMP8 mice to find an invisible platform was impaired compared with that of SAMR1 mice (Fig. 3A and B). The main effect for day was significant ( $F(6,270) = 25.74, p < 0.001$ ). The day × group interaction was not significant ( $F(24,270) = 0.69, p > 0.05$ ). Though the main effect for group was not significant ( $F(4,45) = 1.968, p < 0.05$ ), two-way RM ANOVA revealed a significant increase in escape latency in the vehicle-treated SAMP8 mice when compared with that of SAMR1 mice ( $F(1,20) = 4.4, p < 0.05$ ), and a significant decrease in escape latency in T<sub>4</sub>-treated group (4.0 µg/kg per day) when compared with that of vehicle-treated SAMP8 controls ( $F(1,17) = 4.925, p < 0.05$ ). The significant increase in escape latency in finding the platform in the group of vehicle-treated

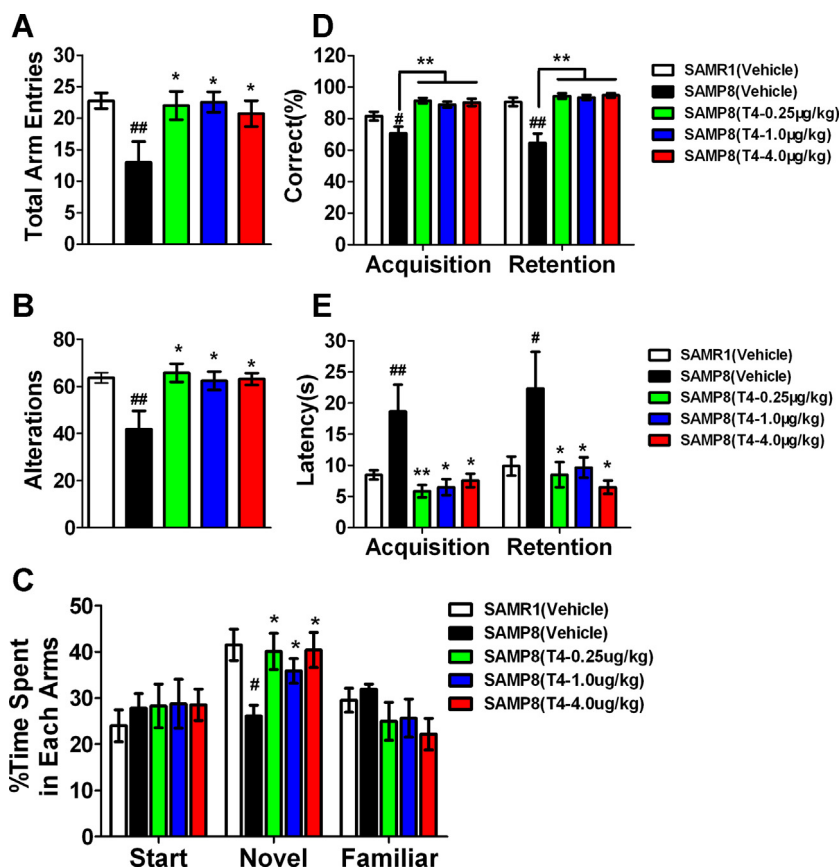


**Fig. 2.** Influence of chronic T<sub>4</sub> treatment on Y-maze performance in aged SAMP8 mice. A battery of behavioral tests representing various cognitive functions was carried out sequentially for 10-month-old male mice. (A) Total arm entries were counted for 8 min. SAMP8 (vehicle) showed fewer total arm entries than did mice given T<sub>4</sub>-0.25, -1.0, -4.0 µg/kg, respectively or SAMR1 mice. (B) Spontaneous alternation (%) was calculated as the ratio of actual alternations to possible alternations. (C) A two-trial recognition Y-maze T<sub>4</sub>-0.25, -1.0, -4.0 µg/kg treated groups showed a significantly higher percentage of entries into the novel arm than into the other arm. (D and E) Contextual conditioned shock-light-dark tasks were performed. A Retention session was carried out 24 h after the shock conditioning. The accuracy rate of T<sub>4</sub>-treated SAMP8 mice was significantly higher than that of SAMP8 (vehicle), and the escape latency was shorter. Each column indicates mean ± S.E. (R1, n = 12; P8 (vehicle), P8 + T<sub>4</sub>-0.25, n = 10; P8 + T<sub>4</sub>-1.0, -4.0 µg/kg, n = 9). <sup>#</sup>p < 0.05, <sup>##</sup>p < 0.01, compared with SAMR1 (vehicle). <sup>\*</sup>p < 0.05, <sup>\*\*</sup>p < 0.01, compared with SAMP8 (vehicle).

SAMP8 controls was observed on day 1 when compared with that of SAMR1 control mice ( $p < 0.05$ ), whereas the significant decrease in escape latency in T<sub>4</sub>-treated groups, as compared with that of aged SAMP8 controls was observed on day 6 and 7 of training ( $p < 0.05$ ). In probe trials, the SAMP8 mice without T<sub>4</sub> treatment failed to show any spatial bias for the platform positions and they spent significantly shorter time in the target quadrant than SAMR1 mice ( $14.03 \pm 4.47\%$  vs.  $28.30 \pm 4.15\%$ ,  $p < 0.05$ ) (Fig. 3C). Meanwhile, the SAMP8 mice with T<sub>4</sub> treatment consistently spent approximately one-third of the probe time searching the quadrant that previously contained the hidden platform. The crossing number of T<sub>4</sub>-treated mice was significantly different from that of the aged SAMP8 control ( $p < 0.05$ ) (Fig. 3D). The crossing number was  $2.6 \pm 0.45$  for the 0.25 µg/kg per day group,  $2.7 \pm 0.36$  for the 1.0 µg/kg per day group, and  $3.14 \pm 0.48$  for the 4.0 µg/kg per day group.

Taken together, these data indicate that the SAMP8 mice consistently display obvious cognitive abnormalities in different learning and memory paradigms, while T<sub>4</sub> treatment improves learning and memory loss in aged SAMP8 mice, although there was no observed significant difference between groups of different dosages in some tests of our study.

### 3.2. T<sub>4</sub> ameliorates hippocampal LTP in aged SAMP8 mice

Synaptic plasticity plays an important role in elucidating the neurobiological mechanisms of learning and memory. We sought

to assess, *in vivo*, whether T<sub>4</sub> rescued the underlying impairment of electrophysiological parameters in aged SAMP8 mice. After behavioral tests, brains were removed from the SAMP8 mice with and without T<sub>4</sub> treatment and LTP was assessed in the CA1 region of the hippocampus. Slices from 10-month-old SAMP8 mice were significantly less responsive to conditioning trains than those from age-matched SAMR1 controls ( $113.85 \pm 6.94\%$  vs.  $148.96 \pm 11.14\%$ ,  $p < 0.01$ ) (Fig. 4). LTP at 60 min after high-frequency stimulus trains was  $148 \pm 7.85\%$  ( $n = 12$ ) for SAMR1 mice and  $115 \pm 7.56\%$  ( $n = 10$ ) for SAMP8 mice (Fig. 4). The two train high frequency stimulation also successfully induced LTP in slices from T<sub>4</sub>-treated SAMP8 mice at 0.25 µg/kg. For these animals, LTP responses between 0 and 60 min after high-frequency stimulus trains was  $124.52 \pm 4.45\%$  and at 60 min was  $125 \pm 3.45\%$  ( $n = 10$ ). The LTP responses of T<sub>4</sub>-treated SAMP8 mice at 1.0 and 4.0 µg/kg were not significantly different from those of age-matched SAMR1 controls ( $141.07 \pm 6.94\%$  vs.  $149.96 \pm 11.14\%$  and  $142.24 \pm 7.22\%$  vs.  $149.96 \pm 11.14\%$ , respectively,  $p > 0.05$ ), whereas they were markedly enhanced compared with those of age-matched SAMP8 mice without T<sub>4</sub> treatment ( $p < 0.01$ ) (Fig. 4). For these animals, LTP at 60 min was  $141 \pm 4.03\%$  for T<sub>4</sub> at 1.0 µg/kg ( $n = 9$ ); and  $140 \pm 5.77\%$  ( $n = 9$ ) for T<sub>4</sub> at 4.0 µg/kg (Fig. 4).

Together with the behavioral data, these electrophysiological data strongly suggest that T<sub>4</sub> can alleviate functional abnormalities and reverse the hippocampal synaptic plasticity impairment in aged SAMP8 mice.

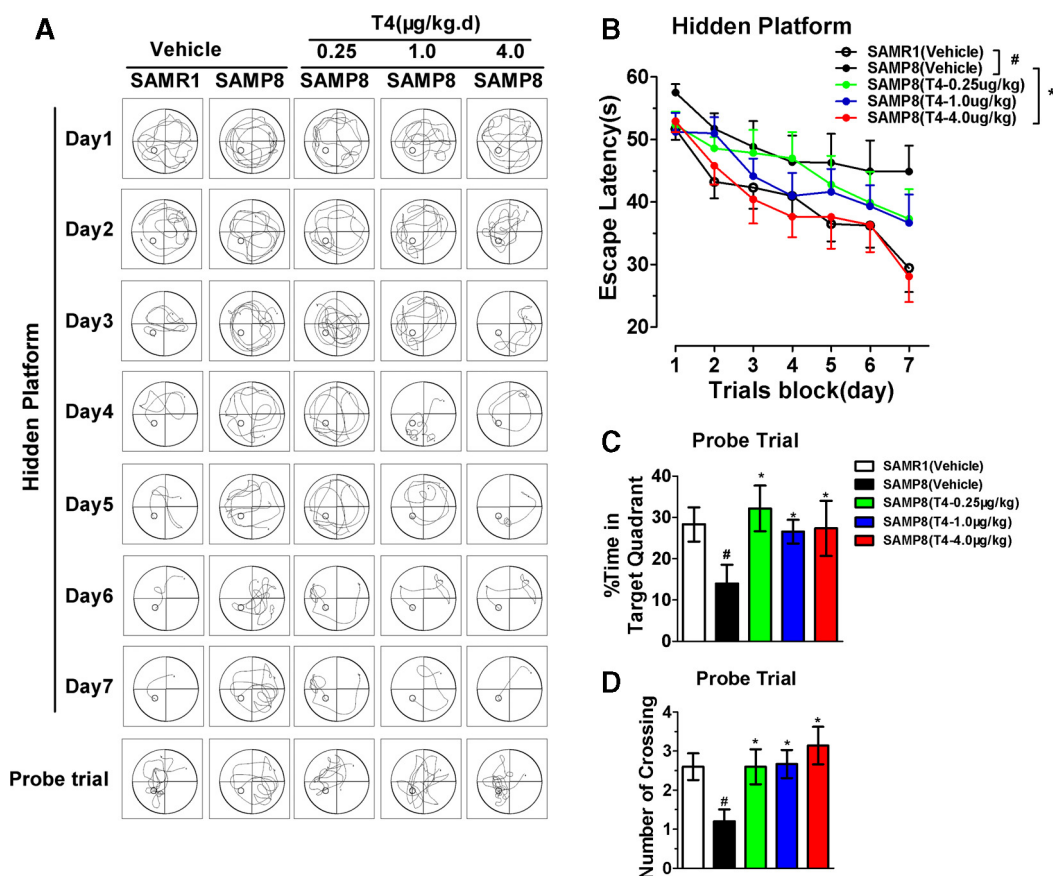


**Fig. 3.**  $T_4$  improves the spatial learning and memory of aged SAMP8 mice in the Morris water maze. Escape latency in each block of the hidden platform during a 60-s session was measured over 7 days in aged SAMP8 at 10 months. The probe test was performed on day 8. (A) Representative swimming tracks showed a block of 4 trials per day in each group. Tracks of the  $T_4$ -0.25, -1.0, -4.0  $\mu\text{g}/\text{kg}$  treated groups showed shorter paths to escape to the hidden platform in a spatial acquisition test (row 1–7) and longer paths to explore the target quadrant, as well as more times crossing the place where the platform was previously located in the probe test (bottom row) than that of SAMP8 (vehicle). (B) The latency in SAMP8 (vehicle) was significantly longer than that of SAMR1 (vehicle) mice. The latencies of  $T_4$ -0.25, -1.0, -4.0  $\mu\text{g}/\text{kg}$  treated groups were significantly shorter than that of SAMP8 (vehicle). Data are expressed as means  $\pm$  S.E. and analyzed by repeated-measure two-way (group  $\times$  day) ANOVA. (C and D) Time mice spent in target quadrant and the number of crossings in the probe test was presented as mean  $\pm$  S.E. One-way ANOVA was performed. #  $p < 0.05$ , compared with SAMP8 (vehicle). \*  $p < 0.05$  or \*\*  $p < 0.01$ , compared with SAMR1 (vehicle).

### 3.3. $T_4$ up-regulates the expression of synapse plasticity-related NMDAR1 and PSD-95 proteins in the hippocampus of SAMP8 mice

Synaptic plasticity is associated with cognition and relies on the normal integration of glutamate receptors at the PSD. We studied the levels of two synaptic proteins, postsynaptic density 95 (PSD95) and p-NMDAR1. As shown in Fig. 5, compared with SAMR1 mice, the expression of PSD-95 and p-NMDAR1 in the hippocampus of the vehicle-treated SAMP8 mice was decreased by 29.6% and 42.2%, respectively. In contrast, compared with that of vehicle-treated SAMP8 group, the expression of PSD-95 and p-NMDAR1 in the hippocampus of  $T_4$ -treated SAMP8 group was respectively significantly up-regulated ( $p < 0.05$ ). The maximal accelerant potency of  $T_4$  at 4.0  $\mu\text{g}/\text{kg}$  per day was 1.8-fold for PSD-95 and 3.2-fold for p-NMDAR1 (Fig. 5).

### 3.4. $T_4$ increases the level of BDNF protein by up-regulating the level of CaMKII and CREB phosphorylation in SAMP8 mice

CaMKII plays a key role in synaptic plasticity, while autophosphorylation of the kinase is essential for NMDAR-dependent LTP [32] in CA1 as part of spatial learning. As shown in Fig. 6A, the level of p-CaMKII decreased by 26.8% in the vehicle-treated SAMP8 mice when compared with that of the SAMR1 mice. However, the p-CaMKII level was significantly upregulated, nearly to the level of SAMR1 mice, when SAMP8 mice were treated with  $T_4$ .

Cyclic AMP-response element binding protein (CREB), which can be phosphorylated by CaMKII, is a transcription factor that binds to the promoter region of many genes, including BDNF, which is associated with memory and synaptic plasticity. Western blot analysis demonstrated that the levels of p-CREB and BDNF proteins were significantly decreased in the hippocampus of vehicle-treated SAMP8 mice (50.0% and 21.4% respectively), when compared with those of SAMR1 mice (Fig. 6A and B). However,  $T_4$  treatment restored the levels of p-CREB and BDNF proteins to those of control SAMR1 mice (Fig. 6B and C). The p-CREB protein level in the  $T_4$ -treated SAMP8 mice (4.0  $\mu\text{g}/\text{kg}$  for 75 days) was found to be significantly increased by nearly 180% when compared with that of the SAMP8 vehicle-treated SAMP8 group and the expression of BDNF was up-regulated close to the level in the SAMR1 mice across the  $T_4$ -treated SAMP8 groups. These data strongly suggest that  $T_4$  alleviates synaptic plasticity dysfunction by triggering the CaMKII-CREB-BDNF signal pathway.

### 3.5. $T_4$ at an optimal dose produces no adverse effects on the survival of mice and no significant drug side-effects on blood counts and blood biochemical changes

The above data clearly demonstrate that  $T_4$  ameliorates the cognitive impairment in SAMP8 mice. We were also interested in whether  $T_4$  could affect the health and/or lifespan of SAMP8 mice. Under the microbiological condition of housing, the life span of

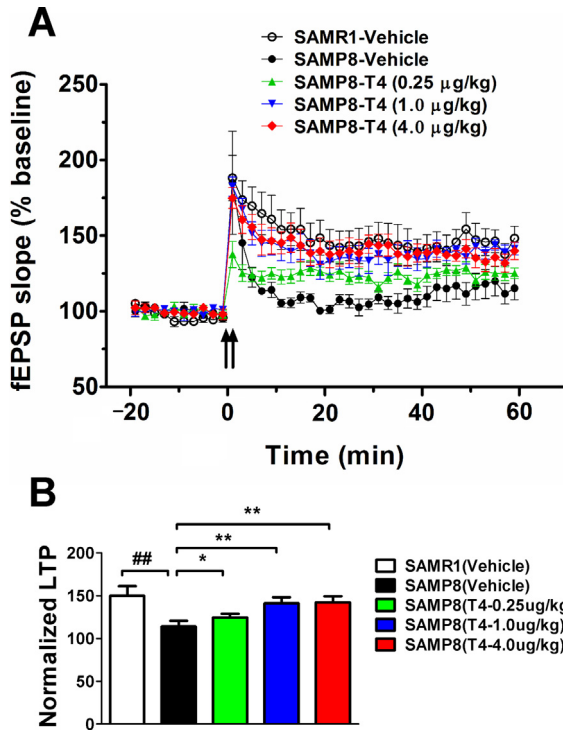


**Fig. 4.** T<sub>4</sub> ameliorates hippocampal LTP in aged SAMP8 mice. (A) LTP was induced by two high-frequency stimulus trains. The level of long-term potentiation was compared between SAMR1 (vehicle), SAMP8 (vehicle) and the T<sub>4</sub> treated group slices. Slices from SAMP8 (vehicle) mice potentiated significantly shorter than those from SAMR1 (vehicle) and the T<sub>4</sub> treated groups. The arrows indicate application time points for conditioning stimulus trains. (B) Statistical analysis of average LTP responses between 0 and 60 min after two high-frequency stimulus trains. Data are expressed as means ± S.E. ##*p* < 0.01, compared with SAMR1 (vehicle). \*\**p* < 0.01, compared with SAMP8 (vehicle).

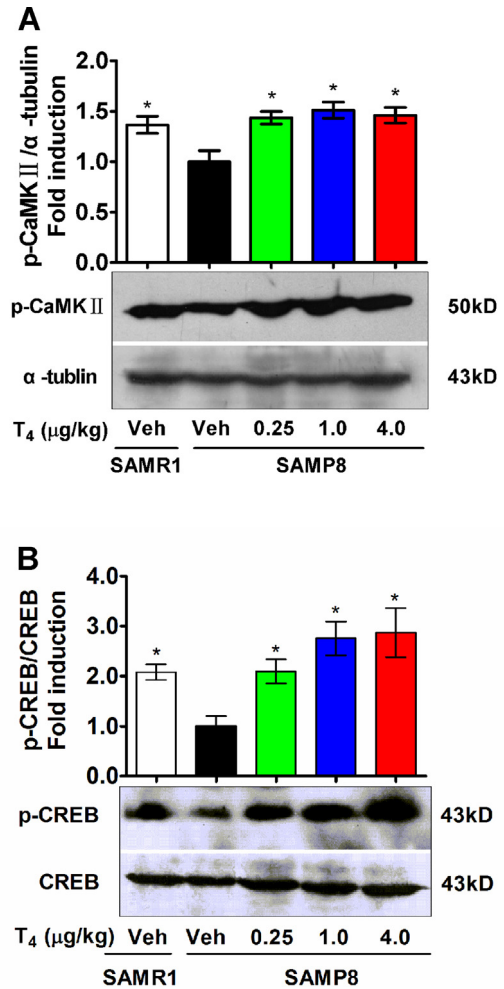


**Fig. 6.** T<sub>4</sub> increases the levels of p-CAMKII, p-CREB and BDNF expression in the hippocampus of SAMP8 mice. The mice were treated with T<sub>4</sub> (0.25, 1.0, or 4.0 μg/kg per day) for 75 days. (A) Representative Western blot for p-CAMKII. α-tubulin was used as a control for protein loading. Densitometric analysis of the p-CAMKII band was normalized to α-tubulin and expressed as relative fold compared with control. (B) Representative Western blot of p-CREB and CREB protein. The amount of phosphorylated CREB and total CREB was quantified by scanning densitometry of immunoreactive bands and expressed as relative fold compared with control. (C) Representative Western blot of BDNF. α-Tubulin was used as a control for protein loading. Densitometric analysis of BDNF band was normalized to α-tubulin and expressed as relative fold compared with control. The values are expressed as mean ± S.E. of at least three independent experiments. \**p* < 0.05, compared with SAMP8 (vehicle).

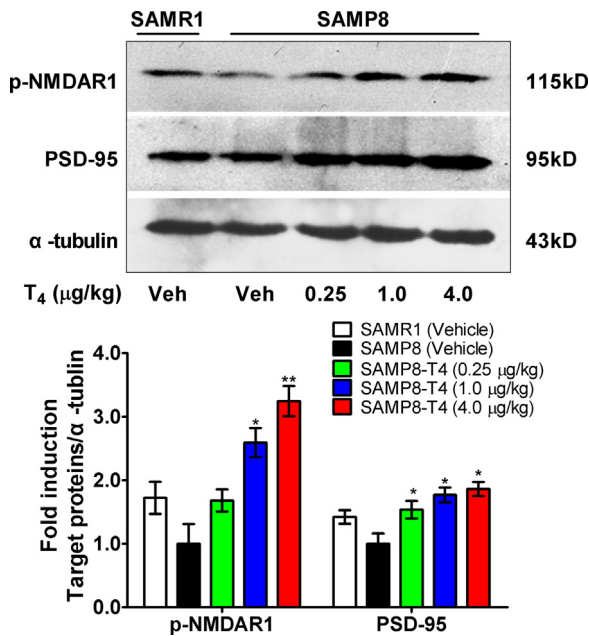


**Fig. 5.** T<sub>4</sub> up-regulates the levels of p-NMDAR1 and PSD-95 in the hippocampus of SAMP8 mice. The mice were treated with T<sub>4</sub> (0.25, 1.0, 4.0 μg/kg per day, respectively) for 75 days. (A) Representative Western blot of p-NMDAR1 and PSD-95. α-Tubulin was used as a control for protein loading. (B) Densitometric analysis of p-NMDAR1 and PSD-95 test bands were normalized to α-tubulin and expressed as relative fold compared with control. The values are expressed as mean ± S.E. of at least three independent experiments. \**p* < 0.05, \*\**p* < 0.01, compared with SAMP8 (vehicle).



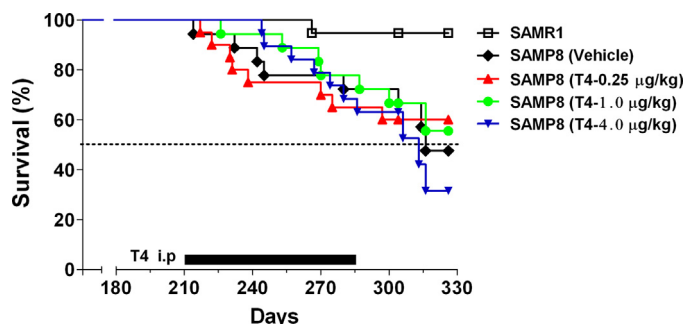


**Fig. 7.** Effects of  $T_4$  treatment on survival of aged SAMP8. Survival curves were plotted for vehicle-treated SAMR1 mice and all SAMP8 groups. Survival curves were analyzed by the *Logrank* test. In contrast to R1, P8 mice that received vehicle showed a decreased survival.  $T_4$  treatment of SAMP8 mice did not result in a decrease in survival ( $p = 0.7325$ ).

SAMP8 mice ranges from 10 months to 17 months. This life span is shorter than that of SAMR1 mice, which ranges from 19 months to 21 months [33]. The analysis of the survival curves showed that there was a markedly higher mortality rate in the SAMP8 mice than in SAMR1 mice (Fig. 7). Only 1 mouse died in the SAMR1 group, but 8 out of 18 in the SAMP8 mice died. The median survival time of the SAMP8 mice from day 1 to sacrifice was 316 days ( $\chi^2 = 7.930$ , vs. SAMR1,  $p = 0.0049$ ). However, by the sacrifice day, the mortality rate in the  $T_4$ -treated groups (0.25, 1.0, 4.0  $\mu\text{g}/\text{kg}$  per day) was 40.0%, 44.4% and 68.4%, respectively. Accordingly,  $T_4$  administration for 75 days did not statistically change the survival rate of the SAMP8 mice under our experimental conditions ( $\chi^2 = 0.6403$ ,  $\nu = 3$ ,  $p = 0.8872$ ) (Fig. 7).

We measured the routine blood counts in all mice to determine the effects of  $T_4$  on peripheral blood in the SAMP8 mice. The results showed that there were no significant changes in the quantity of different leukocytes, or the levels of erythrocytes and platelets between the SAMP8 mice with and without  $T_4$  treatment (Fig. 8,  $p > 0.05$ ). Meanwhile, we also measured blood biochemical indexes including blood plasma protein, transaminases, lipids, glucose, creatinine and cardiac enzymes. Compared with SAMR1 mice, the vehicle-treated SAMP8 group had lower levels of albumin, cholesterol and creatine kinase ( $p < 0.05$ ). However, no significant differences were found in overall biochemical indexes between the SAMP8 mice with  $T_4$  treatment and those without  $T_4$  treatment ( $p > 0.05$ ) (Table 1). These results demonstrate that long-term  $T_4$  administration (0.25, 1.0, 4.0  $\mu\text{g}/\text{kg}$  per day) does not result in significant drug side-effects on blood cells or blood biochemistry.

#### 4. Discussion

According to the related literature available, an extensive characterization of the effects of triphenylmethyl (T<sub>4</sub>), a pharmacological active component purified from the natural product *Tripterygium wilfordii Hook F* (TWHF), has seldom been studied in an Alzheimer's disease mouse model. We have demonstrated in previous studies that *in vitro*,  $T_4$  is neuroprotective against inflammatory neurotoxicity induced by lipopolysaccharide or A $\beta$ -activated microglia by inhibiting NF- $\kappa$ B and JNK signaling [18,19], and neuronal apoptosis induced by A $\beta$  by regulating Wnt/ $\beta$ -catenin signaling [20]. To the best of our knowledge, the current study appears to be a first attempt to show that  $T_4$  *in vivo* promotes synaptic plasticity and subsequently maintains learning and memory capacity in SAMP8 model of AD. This study has identified a novel regulatory mechanism different from the established neuroprotective activity by which  $T_4$  plays a multi-faceted role in preserving synaptic plasticity, including regulation of LTP and balance of synaptic plasticity-related proteins, such as PSD-95, NMDAR, and the related

signal activation. Our results further highlight the potentiality of  $T_4$  treatment for neurodegeneration and conditions involving impaired cognition, with implications for a wider range of CNS disorders.

Most mouse models for AD research currently focus on the expression of AD-related specific gene mutations present in early-onset familial AD and thus represent less than 5% of AD cases. The SAMP8 model, however, has been documented by a considerable number of reports to be a good model for studying the mechanism of age-related cognitive dysfunction displaying many features known to occur early in the pathogenesis of AD, such as increased amyloid- $\beta$  alterations [34], tau hyperphosphorylation, cholinergic system dysfunction [35], noticeable functional deficits in hippocampal and prefrontal cortical circuits and dendritic spine abnormalities in hippocampal neurons [3,4]. Furthermore, the long-term potentiation (LTP) in the CA1 area of hippocampal slices prepared from SAMP8 mice significantly decreased with age [36]. Therefore, SAMP8 mice may be an excellent candidate for studying the early neurodegenerative changes associated with sporadic AD and may provide a more complete picture of a human syndrome triggered by a combination of age-related events.

Different behavioral tests have demonstrated that SAMP8 mice have age-related learning and memory deficits [37–41]. We also found that the aged SAMP8 mice displayed obvious cognitive abnormalities, consistently observed in different learning and memory tests, when compared with the age-matched SAMR1 mice. More importantly, when we explored how an active intervention of  $T_4$  would affect the cognitive deficits in this mouse model, we found that a long-term low dose administration of  $T_4$  (0.25–4.0  $\mu\text{g}/\text{kg}$  per day for 75 days) improved the performance of SAMP8 mice in spatial working memory (the spontaneous alternation behavioral task), visual recognition memory (the two-trial recognition Y-maze), spatial alternation (the contextual conditioned shock-light-dark task) and acquisition and retention of reference memory in Morris water maze task.

In these learning and memory paradigms, spatial memory requires an integrative control function in the hippocampal formation [31] and synaptic plasticity represents a prominent component of this cognitive activity. The hippocampus has therefore been a major experimental system for studies of synaptic plasticity in the context of putative information-storage mechanisms in the brain. Long-term potentiation (LTP) is the main form of synaptic plasticity [42,43], and was first identified in the hippocampus, reflecting the activity level of the synaptic information storage process. Thus, LTP can serve as a promising index to study the underlying mechanisms of learning and memory. In the present study, we demonstrated for the first time that improvement of hippocampal LTP in  $T_4$ -treated SAMP8 mice is dose-dependent, suggesting that  $T_4$  can improve synaptic plasticity in SAMP8 mice. These results also indicate that  $T_4$  can promote synaptic integrity and plasticity, as well as cognitive function.

The prevailing view is that NMDARs play a pivotal role in the induction of many forms of activity-dependent LTP, by acting as a coincidence detector of presynaptic and postsynaptic firing [44]. NMDAR1 subunit dysfunction is linked to cognitive impairment in aged animals [45,46]. NMDA receptors are responsible for most  $\text{Ca}^{2+}$  influx in response to synaptic activity. Since this channel is  $\text{Ca}^{2+}$  permeable, the influx of  $\text{Ca}^{2+}$  can trigger autophosphorylation of CaMKII, promoting translocation of CaMKII to the PSD and interaction with the NMDAR. This leads to activation of intracellular signaling pathways that culminate in the phosphorylation of transcription factors such as CREB, which is critical for LTP [47–50]. CREB phosphorylation plays a key role in synaptic function and memory [51,52]. CREB is a transcription factor binding to the promoter regions of genes, including BDNF, which is associated with memory and synaptic plasticity [53,54]. To date, there have been no

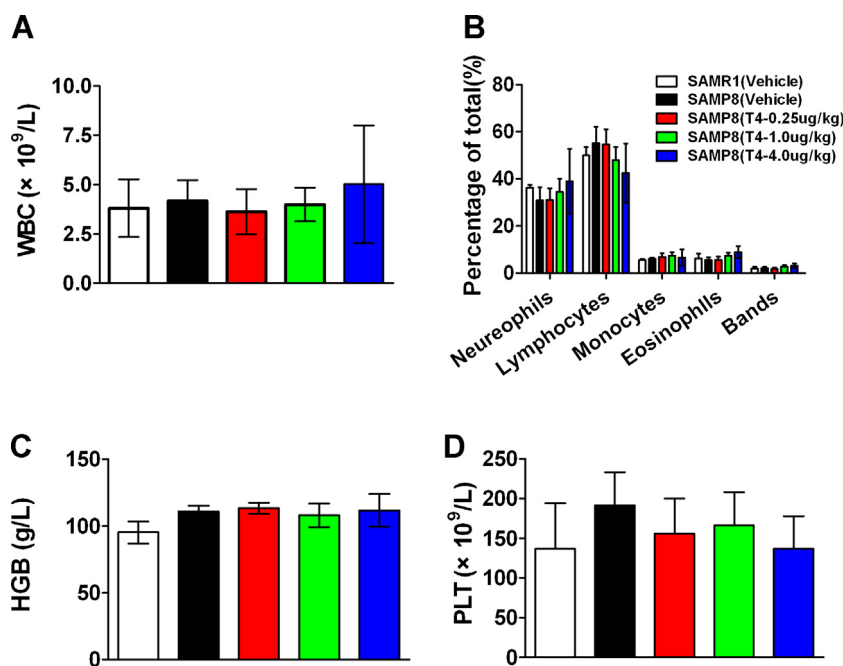


**Fig. 8.** Effects of T<sub>4</sub> on peripheral blood cells in SAMP8 mice. (A and B) Cell counts and categorization of peripheral while blood cells (C) the level of hemoglobin in peripheral red cells. (D) Quantification of blood platelets. Data are expressed as means  $\pm$  S.E. Percentage of various cell types, levels of hemoglobin and platelets from different treated groups were plotted ( $p > 0.05$ ).

**Table 1**  
Effects of T<sub>4</sub> on serum biochemistry indexes in SAMP8 mice.

Biochemistry indexes	R1 (vehicle) N = 12	P8 (vehicle) N = 10	P8 (T4-0.25) N = 10	P8 (T4-1.0) N = 9	P8 (T4-4.0) N = 9
Total protein (g/L)	57.98 $\pm$ 1.01	51.51 $\pm$ 5.83	56.94 $\pm$ 1.30	58.88 $\pm$ 2.48	54.80 $\pm$ 1.42
Albumin (g/L)	33.60 $\pm$ 0.62	26.40 $\pm$ 2.78*	30.06 $\pm$ 0.56	30.32 $\pm$ 0.96	31.16 $\pm$ 1.16
Alanine aminotransferase (ALT) (IU/L)	38.24 $\pm$ 9.22	40.50 $\pm$ 8.58	46.95 $\pm$ 4.52	68.73 $\pm$ 22.85	63.30 $\pm$ 17.19
Aspartate aminotransferase (AST) (IU/L)	125.03 $\pm$ 13.97	95.21 $\pm$ 16.45	140.40 $\pm$ 26.69	81.87 $\pm$ 20.00	131.2 $\pm$ 29.24
Alkaline phosphatase (IU/L)	87.92 $\pm$ 15.63	55.90 $\pm$ 6.90	62.40 $\pm$ 3.46	61.25 $\pm$ 5.19	61.2 $\pm$ 3.78
Cholesterol (mmol/L)	3.22 $\pm$ 0.25	2.07 $\pm$ 0.36*	2.85 $\pm$ 0.28	2.84 $\pm$ 0.10	2.37 $\pm$ 0.48
Triglyceride (mmol/L)	1.10 $\pm$ 0.10	1.20 $\pm$ 0.22	1.85 $\pm$ 0.20	1.51 $\pm$ 0.24	1.75 $\pm$ 0.26
Glucose (mmol/L)	10.65 $\pm$ 0.80	8.45 $\pm$ 1.74	11.82 $\pm$ 1.00	10.12 $\pm$ 1.12	9.35 $\pm$ 2.04
Creatine kinase (U/L)	809.00 $\pm$ 116.59	419.66 $\pm$ 89.19*	802.38 $\pm$ 188.97	628.25 $\pm$ 124.09	764.63 $\pm$ 216.28
Creatine kinase MB mass (U/L)	220.03 $\pm$ 14.26	173.56 $\pm$ 28.86*	217.75 $\pm$ 33.26	244.37 $\pm$ 29.00	231.86 $\pm$ 26.76

Data are expressed as means  $\pm$  S.E. (n = 9–12).

\*  $P < 0.05$ , compared with SAMR1 (vehicle).

reports on the effects of T<sub>4</sub> on the activation of NMDAR-mediated synaptic plasticity. Our results provide the first evidence that systemic long-term delivery of T<sub>4</sub> can enhance the NMDAR-mediated CaMKII-CREB-BDNF synaptic plasticity-related signaling pathway in aged SAMP8 mice.

Substantial data have identified that A $\beta$  may be responsible for synapse loss and dysfunction in AD. At physiological levels, A $\beta$  has an essential function at the synapse. However, in presence of amyloidosis, soluble non-fibrillar A $\beta$  assemblies present in AD brain cause synaptic memory failure [55,56]. The integrity of synapses in mnemonic circuitry is compromised in its structure and function. A $\beta$  has been proved to be a modulator of synaptic plasticity and transmission in AD pathogenesis. Recent data indicate that overproduction of A $\beta$  induces destructive effects in

pre- and post-synapse and that its influence could even be extended over a distance of about 10 microns of neurons to involve more synapses, which interferes more storage of memory and obstructs signals transmission in the brain [57].

In another study of T<sub>4</sub> effects on the production of APP and A $\beta$  proteins, we found, that T<sub>4</sub> decreases the expression of A $\beta$ (1–40) and A $\beta$ (1–42) *in vitro* by modulating  $\beta$ -secretase (BACE1) (paper unpublished, data not shown). We consider T<sub>4</sub> as a modulator of  $\beta$ -secretase in the A $\beta$  production. It was reported that a  $\gamma$ -secretase modulator CHF5074 attenuated memory deficit in young transgenic mice without amyloid-beta plaque deposition. After 4 week of oral treatment with  $\gamma$ -secretase modulator, the impairment of memory was fully reversed, which is also associated with the reversal of LTP impairment in the hippocampus [58].

The result implies that the beneficial effects of modulator of APP secretase may occur at an early stage that precedes the plaque formation.

In present study, T<sub>4</sub> treatment improved the learning and memory functions and reversed the impairment of LTP in SAMP8 mice that were proved to have early amyloid accumulation from 6 months onward [6]. There are grounds for believing that this is a modulated effect by inhibiting A $\beta$  overproduction. It would be more convincing if the intraneuronal A $\beta$  and hyperphosphorylated tau were detected along with the alternations of cognition and neuronal plasticity in our experiment.

As a component of anti-inflammatory drug, T<sub>4</sub> may work not only by lowering the expression of A $\beta$  but also by reducing of inflammation to improve AD thus reversing the cognitive impairment. However, until present, there are only very few reports about anti-inflammation drugs on A $\beta$ -mediated suppression of synaptic plasticity and memory function, let alone specific studies of T<sub>4</sub> effects. Moreover results from different experiments are controversial because of the inconsistent experiment design. One study reported that chronic administration of NSAID indomethacin restored learning deficits and dysfunctional synaptic plasticity induced by aggregated amyloid deposits in the dentate gyrus were restored [59]. It proposed that the inflammatory response by A $\beta$  deposition has a detrimental effect on synaptic function and memory. However, in another study, NSAIDs ibuprofen and naproxen were found to restore memory function in Tg2576 mice and block A $\beta$ -mediated inhibition of LTP in a way other than reductions in the expression of A $\beta$ <sub>42</sub> or decreases in inflammation [60]. With the data we obtained in present study, in order to identify a mechanism underlying the T<sub>4</sub>-induced improvement of the cognitive deficits and synaptic plasticity in AD, further supplementary experiments are needed to differentiate the possible anti-inflammatory regulation pathways and associated inflammation factors including inflammatory cytokines, tumor necrosis factor alpha (TNF- $\alpha$ ) and interleukin 1beta (IL-1 $\beta$ ), etc, which may be relevant to the function of T<sub>4</sub>.

As there are few studies about T<sub>4</sub> as a treatment of AD *in vivo*, we selected our doses of T<sub>4</sub> out of the following considerations. Firstly, we realize that AD is a chronic and advancing disease, which advocates a long-term therapeutic scheme of low dosage to avert the toxicity and side-effects as much as possible. Secondly, in the investigation into T<sub>4</sub> effects on other neurodegenerative diseases, such as in PD mice model [61,62], the dosage of T<sub>4</sub> ranged from 0.5  $\mu$ g/kg for 16 days to 1 mg/kg for 28 days, which proved to be effective and safe. Therefore, we chose the aforementioned treatment scheme in the current study (from 0.25  $\mu$ g/kg to 4.0  $\mu$ g/kg for 75 days). As the safe dosage range of T<sub>4</sub> is quite narrow, there was no significant difference found between each dose in our design (only 2.5 fold), which may be a primary reason for the absence of dose-dependent effects in some tests. For all this, interestingly, we found that the dosage of 4.0  $\mu$ g/kg day was significantly effective in both the Morris water maze and electrophysiology test.

In conclusion, our results clearly demonstrate the protective effect of T<sub>4</sub> treatment on learning/memory in a senescence-accelerated mouse (SAM) model of AD. Notably, T<sub>4</sub> treatment is able to reverse the deterioration of LTP in hippocampal CA1 regions observed in aged SAMP8 mice. The mechanism through which T<sub>4</sub> regulates synaptic plasticity may include activity changes in NMDAR-related signal molecules including PSD-95 protein, phospho-CaMKII, phospho-CREB and BDNF in the hippocampus. In addition, T<sub>4</sub> at an optimal dose does not affect the survival of mice or show significant side-effects on blood counts and blood biochemical changes. This observed T<sub>4</sub>-mediated reversal of age-related synaptic dysfunction and NMDAR signaling deficits strongly suggests that T<sub>4</sub> can halt a key early-stage event in AD. Together with

previous studies, our data indicates that T<sub>4</sub> is a potential therapeutic agent for preventing and slowing AD progression.

## Acknowledgements

This work was supported by National Natural Science Grant of China (81200991), Fujian Province Natural Science Grant (2010J05063), Outstanding Young Persons' Research Program for Higher Education of Fujian Province, China (JA10123), Major Project of Fujian Science and Technology Bureau (2009D061).

## References

- [1] Arai H. Alzheimer's disease neuroimaging initiative and mild cognitive impairment. *Rinsho Shinkeigaku* 2007;47:905–7.
- [2] Takeda T, Hosokawa M, Higuchi K, Hosono M, Akiguchi I, Katoh H. A novel murine model of aging, Senescence-Accelerated Mouse (SAM). *Arch Gerontol Geriatr* 1994;19:185–92.
- [3] del Valle J, Bayod S, Camins A, Beas-Zarate C, Velazquez-Zamora DA, Gonzalez-Burgos I, et al. Dendritic spine abnormalities in hippocampal CA1 pyramidal neurons underlying memory deficits in the SAMP8 mouse model of Alzheimer's disease. *J Alzheimers Dis* 2012;32:233–40.
- [4] Lopez-Ramos JC, Jurado-Parras MT, Sanfeliu C, Acuna-Castroviejo D, Delgado-Garcia JM. Learning capabilities and CA1-prefrontal synaptic plasticity in a mice model of accelerated senescence. *Neurobiol Aging* 2012;33:627, e13–26.
- [5] Tomobe K, Nomura Y. Neurochemistry, neuropathology, and heredity in SAMP8: a mouse model of senescence. *Neurochem Res* 2009;34:660–9.
- [6] Del Valle J, Duran-Vilaregut J, Manich G, Casadesus G, Smith MA, Camins A, et al. Early amyloid accumulation in the hippocampus of SAMP8 mice. *J Alzheimers Dis* 2010;19:1303–15.
- [7] Canudas AM, Gutierrez-Cuesta J, Rodriguez MI, Acuna-Castroviejo D, Sureda FX, Camins A, et al. Hyperphosphorylation of microtubule-associated protein tau in senescence-accelerated mouse (SAM). *Mech Ageing Dev* 2005;126:1300–4.
- [8] Orejana L, Barros-Minones L, Jordan J, Puerta E, Aguirre N. Sildenafil ameliorates cognitive deficits and tau pathology in a senescence-accelerated mouse model. *Neurobiol Aging* 2012;33:625, e11–20.
- [9] Guart A, Lopez-Ramos JC, Munoz MD, Delgado-Garcia JM. Aged wild-type and APP, PS1, and APP+PS1 mice present similar deficits in associative learning and synaptic plasticity independent of amyloid load. *Neurobiol Dis* 2008;30:439–50.
- [10] Kumar VB, Farr SA, Flood JF, Kamlesh V, Franko M, Banks WA, et al. Site-directed antisense oligonucleotide decreases the expression of amyloid precursor protein and reverses deficits in learning and memory in aged SAMP8 mice. *Peptides* 2000;21:1769–75.
- [11] Morley JE, Kumar VB, Bernardo AE, Farr SA, Uezu K, Tumosa N, et al. Beta-amyloid precursor polypeptide in SAMP8 mice affects learning and memory. *Peptides* 2000;21:1761–7.
- [12] Morley JE, Farr SA, Flood JF. Antibody to amyloid beta protein alleviates impaired acquisition, retention, and memory processing in SAMP8 mice. *Neurobiol Learn Mem* 2002;78:125–38.
- [13] Poon HF, Joshi G, Sultana R, Farr SA, Banks WA, Morley JE, et al. Antisense directed at the Abeta region of APP decreases brain oxidative markers in aged senescence accelerated mice. *Brain Res* 2004;1018:86–96.
- [14] Morley JE, Farr SA, Kumar VB, Armbrecht HJ. The SAMP8 mouse: a model to develop therapeutic interventions for Alzheimer's disease. *Curr Pharm Des* 2012;18:1123–30.
- [15] Tao XL. Mechanism of treating rheumatoid arthritis with *Tripterygium wilfordii* hook. II. Effect on PGE2 secretion. *Zhongguo Yi Xue Ke Xue Yuan Xue Bao* 1989;11:36–40.
- [16] Tao X, Cush JJ, Garret M, Lipsky PE. A phase I study of ethyl acetate extract of the chinese antirheumatic herb *Tripterygium wilfordii* Hook F in rheumatoid arthritis. *J Rheumatol* 2001;28:2160–7.
- [17] Yu DQ, Zhang DM, Wang HB, Liang XT. Structure modification of triptolide, a diterpenoid from *Tripterygium wilfordii*. *Yao Xue Xue Bao* 1992;27:830–6.
- [18] Pan XD, Chen XC, Zhu YG, Zhang J, Huang TW, Chen LM, et al. Neuroprotective role of tripchlorolide on inflammatory neurotoxicity induced by lipopolysaccharide-activated microglia. *Biochem Pharmacol* 2008;76:362–72.
- [19] Pan XD, Chen XC, Zhu YG, Chen LM, Zhang J, Huang TW, et al. Tripchlorolide protects neuronal cells from microglia-mediated beta-amyloid neurotoxicity through inhibiting NF-kappaB and JNK signaling. *Glia* 2009;57:1227–38.
- [20] Wu M, Zhu YG, Pan XD, Lin N, Zhang J, Chen XC. [Involvement of Wnt/beta-catenin signaling in tripchlorolide protecting against oligomeric beta-amyloid-(1–42)-induced neuronal apoptosis]. *Yao Xue Xue Bao* 2010;45:853–9.
- [21] Arendt T. Synaptic degeneration in Alzheimer's disease. *Acta Neuropathol* 2009;118:167–79.
- [22] Brewer GJ. Neuronal plasticity and stressor toxicity during aging. *Exp Gerontol* 2000;35:1165–83.
- [23] Shaw KN, Commins S, O'Mara SM. Deficits in spatial learning and synaptic plasticity induced by the rapid and competitive broad-spectrum cyclooxygenase inhibitor ibuprofen are reversed by increasing endogenous brain-derived neurotrophic factor. *Eur J Neurosci* 2003;17:2438–46.

- [24] Andreasson KI, Savonenko A, Videnky S, Goellner JJ, Zhang Y, Shaffer A, et al. Age-dependent cognitive deficits and neuronal apoptosis in cyclooxygenase-2 transgenic mice. *J Neurosci* 2001;21:8198–209.
- [25] Kimura R, Devi L, Ohno M. Partial reduction of BACE1 improves synaptic plasticity, recent and remote memories in Alzheimer's disease transgenic mice. *J Neurochem* 2010;113:248–61.
- [26] Dellu F, Mayo W, Cherkaoui J, Le Moal M, Simon H. A two-trial memory task with automated recording: study in young and aged rats. *Brain Res* 1992;588:132–9.
- [27] Conrad CD. What is the functional significance of chronic stress-induced CA3 dendritic retraction within the hippocampus. *Behav Cogn Neurosci Rev* 2006;5:41–60.
- [28] Dellu F, Fauchey V, Le Moal M, Simon H. Extension of a new two-trial memory task in the rat: influence of environmental context on recognition processes. *Neurobiol Learn Mem* 1997;67:112–20.
- [29] Dellu F, Contarino A, Simon H, Koob GF, Gold LH. Genetic differences in response to novelty and spatial memory using a two-trial recognition task in mice. *Neurobiol Learn Mem* 2000;73:31–48.
- [30] Vorhees CV, Williams MT. Morris water maze: procedures for assessing spatial and related forms of learning and memory. *Nat Protoc* 2006;1:848–58.
- [31] Huang SM, Mouri A, Kokubo H, Nakajima R, Suemoto T, Higuchi M, et al. Nephilysin-sensitive synapse-associated amyloid-beta peptide oligomers impair neuronal plasticity and cognitive function. *J Biol Chem* 2006;281:17941–51.
- [32] Silva AJ, Stevens CF, Tonegawa S, Wang Y. Deficient hippocampal long-term potentiation in alpha-calcium-calmodulin kinase II mutant mice. *Science* 1992;257:201–6.
- [33] Butterfield DA, Poon HF. The senescence-accelerated prone mouse (SAMP8): a model of age-related cognitive decline with relevance to alterations of the gene expression and protein abnormalities in Alzheimer's disease. *Exp Gerontol* 2005;40:774–83.
- [34] Takemura M, Nakamura S, Akiguchi I, Ueno M, Oka N, Ishikawa S, et al. Beta/A4 proteinlike immunoreactive granular structures in the brain of senescence-accelerated mouse. *Am J Pathol* 1993;142:1887–97.
- [35] Strong R, Reddy V, Morley JE. Cholinergic deficits in the septal-hippocampal pathway of the SAM-P/8 senescence accelerated mouse. *Brain Res* 2003;966:150–6.
- [36] Yang S, Qiao H, Wen L, Zhou W, Zhang Y. D-Serine enhances impaired long-term potentiation in CA1 subfield of hippocampal slices from aged senescence-accelerated mouse prone/8. *Neurosci Lett* 2005;379:7–12.
- [37] Yagi H, Katoh S, Akiguchi I, Takeda T. Age-related deterioration of ability of acquisition in memory and learning in senescence accelerated mouse: SAM-P/8 as an animal model of disturbances in recent memory. *Brain Res* 1988;474:86–93.
- [38] Ohta A, Hirano T, Yagi H, Tanaka S, Hosokawa M, Takeda T. Behavioral characteristics of the SAM-P/8 strain in Sidman active avoidance task. *Brain Res* 1989;498:195–8.
- [39] Flood JF, Morley JE. Age-related changes in footshock avoidance acquisition and retention in senescence accelerated mouse (SAM). *Neurobiol Aging* 1993;14:153–7.
- [40] Zhao H, Li Q, Zhang Z, Pei X, Wang J, Li Y. Long-term ginsenoside consumption prevents memory loss in aged SAMP8 mice by decreasing oxidative stress and up-regulating the plasticity-related proteins in hippocampus. *Brain Res* 2009;1256:111–22.
- [41] Shi YQ, Huang TW, Chen LM, Pan XD, Zhang J, Zhu YG, et al. Ginsenoside Rg1 attenuates amyloid-beta content, regulates PKA/CREB activity, and improves cognitive performance in SAMP8 mice. *J Alzheimers Dis* 2010;19:977–89.
- [42] Bliss TV, Gardner-Medwin AR. Long-lasting potentiation of synaptic transmission in the dentate area of the unanaesthetized rabbit following stimulation of the perforant path. *J Physiol* 1973;232:357–74.
- [43] Bliss TV, Lomo T. Long-lasting potentiation of synaptic transmission in the dentate area of the anaesthetized rabbit following stimulation of the perforant path. *J Physiol* 1973;232:331–56.
- [44] Rebola N, Srikumar BN, Mülle C. Activity-dependent synaptic plasticity of NMDA receptors. *J Physiol* 2010;588:93–9.
- [45] Grosshans DR, Clayton DA, Coultrap SJ, Browning MD. LTP leads to rapid surface expression of NMDA but not AMPA receptors in adult rat CA1. *Nat Neurosci* 2002;5:27–33.
- [46] Cheli V, Adrover M, Blanco C, Ferrari C, Cornea A, Pitossi F, et al. Knocking-down the NMDAR1 subunit in a limited amount of neurons in the rat hippocampus impairs learning. *J Neurochem* 2006;97(Suppl. 1):68–73.
- [47] Wayman GA, Lee YS, Tokumitsu H, Silva AJ, Soderling TR. Calmodulin-kinases: modulators of neuronal development and plasticity. *Neuron* 2008;59:914–31.
- [48] Finkbeiner S, Greenberg ME. Ca<sup>2+</sup> channel-regulated neuronal gene expression. *J Neurobiol* 1998;37:171–89.
- [49] West AE, Chen WG, Dalva MB, Dolmetsch RE, Kornhauser JM, Shaywitz AJ, et al. Calcium regulation of neuronal gene expression. *Proc Natl Acad Sci U S A* 2001;98:11024–31.
- [50] Nicoll RA, Roche KW. Long-term potentiation: peeling the onion. *Neuropharmacology* 2013;74:18–22.
- [51] Tully T, Bourtchouladze R, Scott R, Tallman J. Targeting the CREB pathway for memory enhancers. *Nat Rev Drug Discov* 2003;2:267–77.
- [52] Miyashita T, Oda Y, Horiuchi J, Yin JC, Morimoto T, Saitoe M. Mg(2+) block of Drosophila NMDA receptors is required for long-term memory formation and CREB-dependent gene expression. *Neuron* 2012;74:887–98.
- [53] Bimonte HA, Nelson ME, Granholm AC. Age-related deficits as working memory load increases: relationships with growth factors. *Neurobiol Aging* 2003;24:37–48.
- [54] Gomez-Pinilla F, Huie JR, Ying Z, Ferguson AR, Crown ED, Baumbauer KM, et al. BDNF and learning: evidence that instrumental training promotes learning within the spinal cord by up-regulating BDNF expression. *Neuroscience* 2007;148:893–906.
- [55] Klyubin I, Cullen WK, Hu NW, Rowan MJ. Alzheimer's disease Abeta assemblies mediating rapid disruption of synaptic plasticity and memory. *Mol Brain* 2012;5:25.
- [56] Shankar GM, Walsh DM. Alzheimer's disease: synaptic dysfunction and Abeta. *Mol Neurodegener* 2009;4:48.
- [57] Wei W, Nguyen LN, Kessels HW, Hagiwara H, Sisodia S, Malinow R. Amyloid beta from axons and dendrites reduces local spine number and plasticity. *Nat Neurosci* 2010;13:190–6.
- [58] Balducci C, Mehdawy B, Mare L, Giuliani A, Lorenzini L, Sivilia S, et al. The gamma-secretase modulator CHF5074 restores memory and hippocampal synaptic plasticity in plaque-free Tg2576 mice. *J Alzheimers Dis* 2011;24:799–816.
- [59] Stephan A, Laroche S, Davis S. Learning deficits and dysfunctional synaptic plasticity induced by aggregated amyloid deposits in the dentate gyrus are rescued by chronic treatment with indomethacin. *Eur J Neurosci* 2003;17:1921–7.
- [60] Kotilinek LA, Westerman MA, Wang Q, Panizzon K, Lim GP, Simonyi A, et al. Cyclooxygenase-2 inhibition improves amyloid-beta-mediated suppression of memory and synaptic plasticity. *Brain* 2008;131:651–64.
- [61] Li FQ, Cheng XX, Liang XB, Wang XH, Xue B, He QH, et al. Neurotrophic and neuroprotective effects of tripchlorolide, an extract of Chinese herb *Tripterygium wilfordii Hook F*, on dopaminergic neurons. *Exp Neurol* 2003;179:28–37.
- [62] Hong Z, Wang G, Gu J, Pan J, Bai L, Zhang S, et al. Tripchlorolide protects against MPTP-induced neurotoxicity in C57BL/6 mice. *Eur J Neurosci* 2007;26:1500–8.